The Quantum state diffusion model and the driven damped nonlinear oscillator

M. Rigo* [a], G. Alber [b], F. Mota-Furtado [a] and P.F. O'Mahony [a]

[a] *Department of Mathematics, Royal Holloway, University of London Egham, Surrey TW20 OEX, United-Kingdom*

[b] *Theoretische Quantendynamik, Fakultät für Physik, Universität Freiburg D-79104 Freiburg im Breisgau, Germany*

(Accepted for publication Phys. Rev. A)

We consider a driven damped anharmonic oscillator which classically leads to a bistable steady state and to hysteresis. The quantum counterpart for this system has an exact analytical solution in the steady state which does not display any bistability or hysteresis. We use quantum state diffusion theory to describe this system and to provide a new perspective on the lack of hysteresis in the quantum regime so as to study in detail the quantum to classical transition. The analysis is also relevant to measurements of a single periodically driven electron in a Penning trap where hysteresis has been observed.

PACS 03.65.Bz, 42.50.Lc, 05.30Ch

I. INTRODUCTION

Emergence of classical properties through interaction with the environment has been the subject of extensive studies. In this context, a study of simple open quantum systems can provide a clue to understanding the mechanism of the quantum-classical transition. In this paper we wish to study one of the simplest nonlinear quantum systems - the anharmonic oscillator. This system, when it is damped and driven, exhibits different behaviour in the steady state when described either quantum mechanically or classically with the later showing bistability [1,2]. In order to describe the emergence of classicality, such differences have to be clarified and the two results reconciled.

The anharmonic oscillator is of particular interest for several reasons. First, its simplicity allows any complexity related to the model to be avoided. Second, it is the archetypical model for dealing with nonlinearities in quantum mechanics and has been widely used to describe a great variety of systems. In particular, it was introduced by Drummond and Walls [3] to describe dispersive optical bistability and more recently has been used by Bortman and Ron [4,5] to study the relativistic motion of a resonantly driven electron in a Penning trap.

*Email: m.rigo@rhbnc.ac.uk.

Drummond and Walls [3] derived the exact steady state expectations values of the photon distribution function hence showing that in the quantum regime this model does not exhibit bistability or hysteresis. One would expect the classical or quantum results to be recovered in the appropriate limit. For instance, the level of excitation, $\langle a^\dagger a\rangle$, has been used to define such a limit [5]. For low excitation number the quantum result should apply while for high excitation number the classical result is expected to give the correct behavior. This description is reasonable but it does not demonstrate how the transition from classical to quantum occurs when the excitation number takes an intermediate value and whether the system suddenly becomes bistable or whether the bistability appears smoothly.

Drummond and Walls [3] state that the extent to which bistability is observed will depend on the quantum fluctuations, which in turn determine the time for random switching between the two stable states. In this case the classical-quantum transition is of a statistical nature and the classical result appears in the limit where the switching time can be considered very large compared to an observational time.

Bortman and Ron [4,5] presented a quantum-mechanical description of a *single atomic system* which is accessible to experiment [6]. They also state that if one does not deal with the effect of fluctuations upon the two stable states, that is, its influence upon the time scale of the stability, bistability is not destroyed by quantum fluctuations and should be observed even in the case of a low level of excitation. According to this description the system is bistable in both regimes and the observation of bistability thus depends on the experimental set up, with no fundamental restriction on its observation.

Motivated by these controversial points of view of Drummond and Walls [3] and Bortman and Ron [4,5] in this paper the quantum-classical transition of the driven damped anharmonic oscillator is investigated with the help of the quantum state diffusion (QSD) method. In the context of typical quantum optical problems, for example, the QSD method describes the continuous monitoring of the state of a photon source by individual photoelectric detection processes which involve heterodyning with a classical intense photon source [7,8]. However, the QSD method has also been proposed as a phenomenological theoretical description of arbitrary individual quan-

tum measurement processes [9–11]. It has already been demonstrated that the QSD method, considered as a dynamical theory for *single quantum systems*, is a valuable tool in the understanding of the emergence of classical chaos in open quantum systems [12]. Thus it is expected that it will also be useful in obtaining new insights into the connection between classical and quantal behaviour of the driven damped anharmonic oscillator coupled to a reservoir, a physical system whose classical dynamics does not exhibit chaos. This is of particular interest here as this quantum system does not exhibit hysteresis whereas the corresponding classical system does. It will be shown that QSD provides a mechanics for bistable motion in phase space which is consistent with the quantum mechanical steady state result that bistability does not appear for mean values over an ensemble. Furthermore, QSD helps to understand the crucial role played by the physical time scales which characterize the approach to the classical equilibrium positions in phase space and the jumps between these two classically stable equilibrium positions due to quantum fluctuations. In addition, the question is addressed as to what can be measured, in principle, in an experiment [6] on such a system and under what conditions such an experimental observation will yield bistability and hysteresis. Finally the assertions of Drummond-Walls and Bortman-Ron are questioned in the light of QSD.

The paper is organized as follows: In section II, the QSD model is briefly depicted. In section III the anharmonic oscillator model is presented, and a brief review of the classical and quantum results related to bistability in the steady state is provided. Section IV describes the anharmonic oscillator from the point of view of QSD. Finally, section V presents a discussion of the results and our conclusions.

II. QUANTUM STATE DIFFUSION

Open quantum systems are represented by the density operator ρ which evolves in time according to a master equation. The most general master equation in the Markov approximation, which preserves trace and positivity of the density operator ρ can be written in the Lindblad form [13]

$$\dot{\rho} = -\frac{i}{\hbar}[H,\rho] + \sum_j \left(L_j \rho L_j^\dagger - \frac{1}{2} L_j^\dagger L_j \rho - \frac{1}{2} \rho L_j^\dagger L_j \right) \quad (1)$$

where H is the Hamiltonian and L_j are Lindblad operators which represent the effects of the environment on the system.

The quantum state diffusion model (QSD) represents one of the several possible unravellings of the master equation. According to the QSD model [9–11,15,16], open quantum systems are represented by pure states $|\psi\rangle$, which describe individual systems. Evolution of the state $|\psi\rangle$ is given by a Langevin-Itô differential equation

$$\begin{aligned} |d\psi\rangle = & -\frac{i}{\hbar} H|\psi\rangle dt \\ & -\frac{1}{2}\sum_j (L_j^\dagger L_j + \langle L_j^\dagger\rangle\langle L_j\rangle - 2\langle L_j^\dagger\rangle L_j)|\psi\rangle dt \\ & +\sum_j (L_j - \langle L_j\rangle)|\psi\rangle d\xi_j. \end{aligned} \quad (2)$$

The $d\xi_j$ are random differential variables representing independent complex Wiener processes. They satisfy the following mean relationships

$$M(d\xi_j) = M(d\xi_j d\xi_k) = 0, \qquad M(d\xi_j d\xi_k^*) = \delta_{jk} dt. \quad (3)$$

M represents a mean over an ensemble and $\langle L_j\rangle = \langle\psi|L_j|\psi\rangle$ the quantum expectation of the operator L_j in the pure state $|\psi\rangle$.

The QSD trajectories are compatible with the master equation in the sense that the ensemble average of the projector $|\psi\rangle\langle\psi|$ reproduces the density operator ρ:

$$\rho = M(|\psi\rangle\langle\psi|). \quad (4)$$

Thus, expectations values $\langle A\rangle_\rho = \mathrm{Tr}(\rho A)$ of an operator A can be computed as the ensemble mean of the quantum expectations values $\langle A\rangle_\psi$ of the pure state $|\psi\rangle$.

III. ANHARMONIC OSCILLATOR

We consider a driven anharmonic oscillator coupled to a thermal bath [3,17–19], the temperature of which is set to zero ($T = 0$) as the prototype model showing bistability in the classical domain. The damping of this oscillator with rate κ, is described by the Lindblad operator $L = \sqrt{\kappa}a$. The Hamiltonian in a frame rotating with the frequency ω of the driving field reads

$$H = \hbar\Delta\omega a^\dagger a + \hbar\beta(a^\dagger + a) + \hbar\chi(a^\dagger a)^2 \quad (5)$$

where $a = (\frac{m\omega_0}{2\hbar})^{1/2} Q + i(\frac{1}{2m\hbar\omega_0})^{1/2} P$ and $a^\dagger$ are the annihilation and creation operators related to the position Q and momentum P of the oscillator (m is the mass of the particle). Here the parameter $\Delta\omega = \omega_0 - \omega$ measures the detuning between the eigenfrequency of the oscillator and the driving force. The parameters β and χ characterize the amplitude of the driving force the strength of the anharmonicity. In the following only positive values of χ will be considered.

This Hamiltonian whose corresponding classical dynamics is integrable is well known. It has been used to describe various physical phenomena such as dispersive optical bistability [3,20], driven tunneling [21] and hysteresis in an atomic system [4,5] within the framework of the rotating wave approximation. In the context of optical bistability, for example, the QSD equation with Hamiltonian (5) and $L = \sqrt{\kappa}a$ describes the continuous monitoring of the electromagnetic field of frequency ω_0 by

individual photon detection processes which involve heterodyning with a classical intense photon source. Without the adiabatic approximation (i.e. for a time dependent driving β) this physical system has been discussed as a model which exhibits quantum chaos [12]. It has also been used to describe more fundamental aspects like the effect of non linearities in master equations [17], non-Markovian approximations [18], and more recently in a study of localization processes [22]. An appealing feature of this system is that exact quantum results exist for the correlations function [3], the spectrum, and even the dynamics [19,23] in the absence of driving.

The classical equivalent for this system exhibits hysteresis in the steady state [1,2] while the quantum system does not. In the next two sections well known results regarding the classical and quantum systems are presented in order to make this presentation self consistent.

A. The classical limit

The classical equation of motion can be obtained [3] by factorizing the quantum correlation functions $\langle a^\dagger a^2\rangle \to \langle a^\dagger\rangle\langle a\rangle^2$

$$\frac{d\alpha}{dt} = -i\left\{\beta + (\Delta\omega+\chi)\alpha + 2\chi\alpha^2\alpha^*\right\} - \frac{1}{2}\kappa\alpha \qquad (6)$$

where α is the mean field amplitude $\alpha = \langle a\rangle$ in the (semi-) classical limit.

In the steady state regime, the excitation number $|\alpha|^2$ can be obtained by solving the following equation

$$|\alpha|^2 = \frac{\beta^2}{(\kappa/2)^2 + (\Delta\omega + \chi + 2\chi|\alpha|^2)^2}. \qquad (7)$$

Once the excitation number $|\alpha|^2$ is known the real and complex part of the mean amplitude α can be derived using

$$\frac{Re(\alpha)}{|\alpha|^2} = \frac{\Delta\omega+\chi+2\chi|\alpha|^2}{\beta}, \qquad \frac{Im(\alpha)}{|\alpha|^2} = -\frac{\kappa}{2\beta}. \quad (8)$$

Expression (7) shows that the classical anharmonic oscillator can display one, two or three solutions depending on the choice of parameter values (see figure 1).

Provided the following conditions are fulfilled

$$\begin{gathered}\chi(\Delta\omega+\chi) < 0 \\ \left|\frac{\Delta\omega+\chi}{\kappa/2}\right| > \sqrt{3} \\ \left[\frac{27\chi\beta^2}{(\Delta\omega+\chi)^3} + 1 + \left(\frac{3\kappa/2}{\Delta\omega+\chi}\right)^2\right]^2 < \left[1 - 3\left(\frac{\kappa/2}{\Delta\omega+\chi}\right)^2\right]^3\end{gathered} \qquad (9)$$

then equation (7) has three solutions. Outside of this range, only one solution is expected.

The first condition expresses the fact that the detuning has to be oriented in the right direction in order to combine its effect with that of the anharmonicity. The second shows that detuning and anharmonicity must be large enough in order to compensate dissipation, and the third condition gives limiting values for the driving strength.

Using the theory of linear stability [3,1], it can be verified that when three solutions are present, one of them is always unstable. Thus the domain of parameters is divided into two regions, one showing bistability and the other purely mono-stable behaviour (see figure 2). In short, the classical model exhibits a bistable steady state when the parameters satisfy the above conditions leading to hysteresis.

B. The quantum limit

Using the complex P representation, Drummond and Walls [3] have solved the master equation for the density operator. They obtained an analytical expression for the moments $\langle a^{\dagger n} a^m\rangle_\rho$ in the steady state. Notice that in this section, the brackets $\langle\cdots\rangle_\rho$ represent the ensemble mean of the quantum mechanical expectation values. Their result reads

$$\langle a^{\dagger n} a^m\rangle_\rho = \left(\frac{z}{2}\right)^{\frac{n+m}{2}} \frac{\Gamma(c)\Gamma(c^*)}{\Gamma(c+m)\Gamma(c^*+n)} \times \frac{F(c+m, c^*+n, z)}{F(c, c^*, z)} \qquad (10)$$

where Γ is the Gamma function and $F \equiv {}_0F_2$ the generalized Gauss hypergeometric series [24]:

$${}_0F_2(c,d,z) = \sum_{n=0}^{\infty} \frac{z^n}{n!}\frac{\Gamma(c)\Gamma(d)}{\Gamma(c+n)\Gamma(d+n)}. \qquad (11)$$

The coefficients c and z depend on the physical parameters in the following way $c = (\Delta\omega+\chi)/\chi - i\kappa/(2\chi)$ and $z = 2(\beta/\chi)^2$.

The mean excitation number is of particular interest here, it is given by

$$\langle a^\dagger a\rangle_\rho = \frac{\beta^2}{(\Delta\omega+\chi)^2 + (\kappa/2)^2}\frac{F(c+1, c^*+1, z)}{F(c, c^*, z)}. \quad (12)$$

Using the properties of the hypergeometric series ${}_0F_2$ one can show that the quantum result is never bistable and thus does not show any hysteresis (figure 1).

IV. QSD FOR THE ANHARMONIC OSCILLATOR

In this section, the problem is tackled using the quantum state diffusion (QSD) model. According to QSD, the equation of motion for the mean field amplitude $\langle a\rangle$ is

$$d\langle a\rangle = -i\left[(\Delta\omega+\chi)\langle a\rangle + \beta + 2\chi\langle a^\dagger a^2\rangle\right]dt - \frac{\kappa}{2}\langle a\rangle dt + \sqrt{\kappa}(\langle a^2\rangle - \langle a\rangle^2)d\xi + \sqrt{\kappa}(\langle a^\dagger a\rangle - \langle a^\dagger\rangle\langle a\rangle)d\xi^*. \quad (13)$$

In this equation, the expectation values are taken in the pure state $|\psi\rangle$ describing the evolution along a quantum trajectory. If one wants to describe the evolution of the mean value (over an ensemble), one can take the mean on both sides of the equation (13) to obtain

$$\frac{d\langle a\rangle_\rho}{dt} = -i\left[(\Delta\omega+\chi)\langle a\rangle_\rho + \beta + 2\chi\langle a^\dagger a^2\rangle_\rho\right] - \frac{\kappa}{2}\langle a\rangle_\rho \quad (14)$$

One can check easily that factorizing the quantum correlations in both of the two preceding equations leads to the classical equation of motion (6). Thus, neglecting the quantum correlations corresponds to ignoring overlapping effects of the wave packet and quantum fluctuations.

A. Simulation of the dissipative dynamics

The parameters are chosen in the bistable domain. The dynamical evolution of the QSD equation (13) is computed numerically using the moving basis or mixed representation simulation method (MQSD) [14]. The evolution is computed over a period of time of the order of $1/\kappa$, *the dissipative time*. In this situation, the system evolves toward a different "stationary" state depending on the chosen initial state. The QSD evolution shows two different limit points where all the trajectories tend to go after some transient dissipative time. These two points are called equilibrium points.

When the trajectory starts far away from the two equilibrium points, it approaches one of them, depending in which basin of attraction it starts in, rotating with a frequency given by the detuning $\Delta\omega$. If the wave packet is initially spread out, it tends to localize [15] to a coherent state during the dissipative transient. Here the state is said to be localized if its spread is much smaller than the distance between the two equilibrium points. Thus the quantum fluctuations have less and less effect.

After the transient damped motion towards one of the equilibrium points, the wave packet remains localized. This strong localization property allows one to describe the quantum system in a quasi classical way.

As a consequence of the anharmonicity, the system does not however preserve the coherent states to which it is driven by the dissipative terms. Hence, the quantum correlations never vanish, and the quantum fluctuations act on the wave packet whose center will fluctuate around it's equilibrium point. The dynamics are now dominated by quantum fluctuations.

These fluctuations have a mean frequency and an amplitude which depends on the position of the equilibrium point in phase space. The fluctuations are bigger for the equilibrium point situated further away from the origin. This is an effect due to dissipation, represented by $L = \sqrt{\kappa}a$, which produces a dynamical behaviour like $\langle\dot{a}\rangle \simeq -\kappa\langle a\rangle$ clearly attracting the system towards the origin $\langle a\rangle = 0$ and not to some local minima.

At this point the QSD trajectories can be roughly seen as classical trajectories subjected to noise. There are two distinct equilibrium points leading to bistable behaviour similar to the classical one.

B. Recovery of the quantum result

We know that the QSD model reproduces the quantum result in mean over an ensemble but if QSD shows bistability, how can the quantum result be recovered ? The answer is that the evolution described above is stable over a very long time compared to the dissipative time, but if one integrates over a longer time, one sees that any trajectory goes from the neighborhood of one equilibrium point to the other. This transition happens in mean after a time called the *transition time* or *exit time*, which can be much longer than the dissipative time.

In order to observe the transition between the two equilibrium points, the parameters are chosen such that the maximal excitation number is set at an intermediate value between the classical and quantum limits. Also, the integration is now carried over a long time, typically 10^2 to 10^4 times the dissipative time. The system is initially set in a coherent state centered far away from the two fixed points and evolved in time with QSD. Figure 3 represents a trajectory in phase space which shows the dissipative part of the trajectory, followed by a long period of fluctuations around the attracting equilibrium point. This first part of the time evolution of the trajectory, i.e. its approach to equilibrium, has been described in the previous section IV A. If the integration is carried on, the trajectory will suddenly jump to the neighbourhood of the other equilibrium point. (The "jump" described here is a diffusive process which allows the quantum trajectory to go from the basin of attraction of one equilibrium point to the other.) The system will remain around the second equilibrium point during some time and then come back to the first point. The time spent around each equilibrium point is such that the quantum expectation value $\langle a\rangle_\rho$ is recovered in mean. Due to quantum fluctuations induced by the coupling to the reservoir the equilibrium points become metastable.

This transition, which occurs in a time shorter than the dissipative time, might be viewed as a tunneling process. Savage and Cheng [21] have investigated whether bistability can be associated with quantum superpositions of states in either well. They have introduced a distinction between coherent and diffusive mechanisms for quantum tunneling. In our simulations, the wave packet initially localized in one well becomes delocalized when it crosses

the barrier, making the distinction between these two mechanisms of tunneling artificial (see figure 4). Once the barrier is crossed, the wave packet localizes again.

To confirm the previous description, a mean over an ensemble is considered. Figure 5 represents the time evolution of the mean position and mean momentum. The mean is computed over 100 trajectories. The system is initially placed in a coherent state centered at the classical equilibrium point. This point is unstable with respect to the other equilibrium point. The mean position and momentum evolve, roughly as an exponential decay, to the quantum stationary values given by the exact quantum result. For this typical example, the quantum result is very close to one of the equilibrium points, because the transition time from the initial to the final point is much shorter than in the opposite direction.

Hence, the mean result confirms that the initial equilibrium point is unstable compared to the other one as a consequence of the quantum fluctuations. This relative instability explains why the quantum description does not show bistability. According to QSD even in the quantum regime, the system is bistable, but the bistability is hidden by the fluctuations which make the wave packet move from a fairly localized state in one well to a localized state in the other well.

V. DISCUSSION

We have used QSD to describe the driven damped anharmonic oscillator in an intermediate regime between quantum and classical. It has been shown that states localize along a quantum trajectory and a transition between the two equilibrium points of the system has been observed. The localization gives a quantitative justification for the classical analogy in which a localized particle moves in a double well potential. This analogy has often been used on a purely qualitative level without any further justification. The transition between the two equilibrium points allows one to recover the quantum result and reconciles quantum and classical descriptions. It is worth emphasizing the following aspects:

A. Transition time

The QSD model, by introducing quantum fluctuations in an explicit way, shows explicitly how classical bistability disappears. Furthermore it introduces a new time scale, the transition time characteristic of the transition between the two (classical) equilibrium points. More precisely there are two transitions times, the transition time from one equilibrium point to the other and a different time associated with the reverse transition. Because one of these transition times is in general much smaller than the other one, the transition considered here starts from the less stable equilibrium point which is located further away from the origin in phase space.

In a sequence of papers, Vogel and Risken [20] have calculated the transition rates by solving the equations of motion for quasidistribution functions using the matrix continued-fraction method. They also obtained analytical results for the transition rate in the limit of large excitation numbers and low damping.

The rate of decay shown on the figure 5 is an approximation to the mean transition rate between the two equilibrium points. The time needed for the decay is clearly much larger than the dissipative time.

Thus QSD not only gives a qualitative description but can also be used easily to obtain numerical estimates of the relevant transition times. We will not address any further the question of the determination of the transition time in this paper as one can use the accurate results of Vogel and Risken which confirm the possibility of very large transition times compared to the dissipative time.

B. Ideal experiment

Let us consider the following ideal experiment : (see [6] for a practical realization) In order to see hysteresis a single quantum mechanical anharmonic oscillator is measured continuously under conditions in which its classical counterpart would be bistable. Let us assume that the driving frequency ω is varied step by step from low to high frequencies and reversed, spanning twice the classically bistable domain. Once the frequency is modified, the experimenter waits a time, called *the measurement delay* t_m, which is assumed to be much longer than the dissipative time, before doing any further measurement. The excitation number of the oscillator is measured before changing the frequency of the driving force again. Thus this type of resonance experiment corresponds to an adiabatic sweeping of the frequency with respect to the "fast" dissipative dynamics. Furthermore, let us assume that this continuous measurement is ideal in the sense that the excitation number of the harmonic oscillator can be measured nondestructively and that it does not perturb the systems transition rates, i.e. it is a nondemolition measurement. Such a measurement can be performed, for example, in an optically bistable system by monitoring the state of the field mode by heterodyning with an intense classical photon source. Alternatively, this measurement can also be realized by observing the relativistic motion of a resonantly driven electron in a Penning trap, like in the recently performed experiment of Ref. [6].

According to QSD such a measurement should reproduce the curve depicted in figure 6 showing hysteresis. The experimenter should obtain such a curve fluctuating around one of the two classical steady state values for a while and then jumping to the other value. The combination of the two jumps occurring when the driv-

ing frequency is ramped from low to high frequencies and reversed allows one to define the detuning width $\Delta\Omega$ as the size of the bistable region. Figure 6 represents such a result and shows the detuning width $\Delta\Omega$ for this particular realization. The detuning width is different for each realization of this experiment, the transition being a stochastic event.

An experiment carried out in the classical limit does not show any fluctuations and the two jumps occur always at the same detuning value. In this case the detuning width $\Delta\Omega$ corresponds to the full size of the bistable region.

If one uses the density matrix to describe such an ideal experiment, the result will also show two distinct transitions. The mean detuning width depends not only on the characteristic physical parameters of the driven damped anharmonic oscillator but also on the measurement delay t_m. If the mean transition time τ is much larger than the dissipative time, i.e. $\tau \gg 1/\kappa$, one can distinguish between the two limiting cases: (1) If the measurement delay is small relative to the transition time, i.e. $\tau \gg t_m$, then the mean detuning width $\Delta\Omega$ has a finite value, showing bistability. (2) At the opposite extreme, i.e. for $t_m \gg \tau$, the detuning width is equal to zero, showing no hysteresis at all, in agreement with the quantum steady state result.

C. Bistability and the classical limit

The classical limit is valid for high excitation number. In this limit the mean transition time is so large and the transition between the two equilibrium points so infrequent that they can be neglected. In this limit any finite observational time satisfies the conditions for the experimental observation of hysteresis.

When the excitation number decreases sufficiently for the mean transition time to take a very large but accessible value, one has to distinguish between the cases where the measurement delay is smaller or larger than the transition time. The classical description is still valid in the former case but does not apply anymore in the latter. The fluctuations have to be taken into account for a correct description of this situation.

If we continue lowering the excitation number, still keeping the mean transition time large compared to the dissipative relaxation time, then the classical theory no longer gives a good description of the dynamics since even for a measurement delay much smaller than the transition time it predicts a fixed detuning width. If one uses quantum theory, which includes the fluctuations, one will be able to obtain the correct behaviour.

Finally when the excitation number is small, the classical theory is no longer valid. One has to use the quantum theory and specify the measurement delay in order to describe correctly the result of an experiment. The bistability is not destroyed in any of these cases but it is simply hidden by the quantum fluctuations.

This situation is very similar to that of a classical driven anharmonic oscillator coupled with a thermal bath with non-zero temperature. Introducing thermal fluctuations also hides the bistability of the steady state and introduces a classical transition time (see [25]). In order to observe bistability, one has to introduce a measurement delay much larger than the relaxation time in the absence of thermal fluctuations, but shorter than the mean transition time. The thermal fluctuation can be neglected only when the transitions take place in a time much larger than the observational time.

In all the previous situations the quantum theory applies. Because the density matrix automatically includes the mean over an ensemble, there is no clear distinction between the dissipative dynamics and the dynamics induced by the fluctuations. QSD, by unraveling the different quantum trajectories, helps one to understand the role played by the statistical mean.

VI. SUMMARY

We have shown that QSD leads to quantum trajectories which exhibit bistability for the driven damped anharmonic oscillator and that the quantum steady state result is recovered through random switching between the two equilibrium points due to quantum fluctuations. The fluctuations also introduce a characteristic time scale: the mean transition time.

We have also shown that it is still possible to observe bistability dynamically in this quantum system by introducing a measurement delay t_m. An experiment will show hysteresis only if the transition time between the (classical) equilibrium points, τ, is much larger than all other relaxation times involved (approximately $1/\kappa$). If the transition time is not that large, it is not possible to observe any hysteresis effects and the quantum steady state solution is expected. Furthermore, provided the transition time is much larger than the other times, hysteresis can be seen only if a measurement delay is such that $t_m \ll \tau$. Thus, within this interpretation the classical result is valid only if the quantum fluctuations are so small that they induce a transition time very large compared to the period of observation.

Our results confirm the statistical description given by Drummond and Walls. The results of Bortman and Ron have to be examined more carefully. Strictly speaking, even for low excitation number, the bistability is not destroyed, it is just hidden by the quantum fluctuations. But one cannot neglect the effect of the fluctuations upon the two stable states since it is exactly these fluctuations which prevent an experimental observation of hysteresis in the steady state.

Finally, if QSD is used to describe the dynamical behaviour of a single quantum system our investigations might be of particular relevance for experiments on opti-

cal bistability or for the recently performed experiments of Gabrielse et al. [6] in which hysteresis was observed.

ACKNOWLEDGMENTS

It is a pleasure to acknowledge very stimulating discussions with Todd Brun, Nicolas Gisin and Rüdiger Schack. Financial support by the EU under its Human Capital and Mobility Programme and the Deutsche Forschungsgemeinschaft is gratefully acknowledged. FMF and PFOM also acknowledge financial support from the PRAXIS XXI programme of the Junta Nacional de Investigacao Cientifica e Tecnologica (JNICT), Portugal.

[1] L.D. Landau and E.M. Lifshitz, *Mechanics*, (Pergamon, New-York,1976).
[2] A.E. Kaplan, Phys. Rev. Lett. **48**, 138, (1982).
[3] P.D. Drummond and D.F. Walls, J. Phys. A**13**, 725, (1980).
[4] D. Bortman and A. Ron, Optics Commun. **108**, 253. (1994).
[5] D. Bortman and A. Ron, Phys. Rev. A**52**, 3316, (1995).
[6] C.H. Tseng and G. Gabrielse, Appl. Phys. B**60**, 95, (1995).
[7] H.Carmichael, *An Open Systems Approach to Quantum Optics*, Lecture Notes in Physics **m18** (Springer, Berlin, 1993)
[8] H.M.Wiseman and G.J.Milburn, Phys.Rev.A **47**, 1652 (1993)
[9] N. Gisin and I.C. Percival, J. Phys. A**25**, 5677, (1992).
[10] N. Gisin and I.C. Percival, J. Phys. A**26**, 2233, (1993).
[11] N. Gisin and I.C. Percival, J. Phys. A**26**, 2245, (1993).
[12] T.P. Spiller and J.F. Ralph, Phys. Lett. A**194**, 235, (1994).
[13] G. Lindblad, Commun. Math. Physics **48**, 119, (1976).
[14] R. Schack, T.A. Brun and I.C. Percival, J. Phys. A**28**, 5401, (1995).
[15] T. Steimle, G. Alber and I.C. Percival, J. Phys. A**28**, L491, (1995).
[16] I.C. Percival, J. Phys. A**27**, 1003, (1994).
[17] F. Haake, H. Risken, C. Savage and D. Walls, Phys. Rev. A**34**, 3969, (1986).
[18] R. Alicki, Phys. Rev. A**40**, 4077, (1989).
[19] G.J. Milburn and C.A. Holmes, Phys. Rev. Lett. **56**, 2237, (1986).
[20] K. Vogel and H. Risken, Phys. Rev. A**42**, 627, (1990) and references therein.
[21] C.M. Savage and W.A. Cheng, Optics Commun. **70**, 439, (1989).
[22] B.M. Garraway and P.L. Knight Optics Commun. **123**, 517, (1996).
[23] F.X. Kärtner and A. Schenzle, Phys. Rev. A**48**, 1009, (1993).
[24] Y.L. Luke, *The Special Functions and Their Approximations*, Vol I and II, (Academic Press, New York,1969).
[25] M.I. Dykman and M.A. Krivoglaz, Physica A**104**, 480, (1980).

FIG. 1. Steady state excitation number $|\alpha|^2$ (classical result - dots) and $\langle a^\dagger a\rangle$ (quantum result - line) versus the detuning $\Delta\omega$. The parameters are: the damping $\kappa = 1.5$, the driving $\beta = -7.0$ (choosing β real is equivalent to setting the origin for the phase of $\langle a\rangle$, introducing a complex β simply produces a rotation in phase space) and the anharmonicity $\chi = 0.05$.

FIG. 2. Representation of the domain of hysteresis. The three conditions given by Eqn.(9) in the text describe the border of this domain. Inside the bounded region the system possesses three solutions, two stable and one unstable, this is the bistable domain. Outside, the system has only one solution, always stable. Notice that the bistable region is entirely defined by only two parameters $x = \frac{\kappa/2}{\Delta\omega+\chi}$ and $y = \frac{(\kappa/2)^3}{\beta^2\chi}$.

FIG. 3. Evolution of a quantum trajectory in phase space. The parameters are: $\kappa = 1.5$, $\beta = -7.0$, $\chi = 0.05$ and the detuning $\Delta\omega = -5.0$. The initial state is chosen to be a coherent state centered at ($\langle Q\rangle = 7, \langle P\rangle = 14$). The first stage of the evolution is the decay towards a local minimum, in a time of the order of $1/\kappa$. Then the system fluctuates around the equilibrium point for an amount of time given, in mean, by the transition time. Finally, a big enough fluctuation occurs to project the system into the other basin of attraction where the system remains for a very long time.

FIG. 4. Representation in time of A) the position $\langle Q\rangle$ (full line) and its variance ΔQ^2 (dotted line) and B) the momentum $\langle P\rangle$ (full line) and its variance ΔP^2 (dotted line) at the particular instant of the transition (approximatively at $t = 596.3$ in this example). Same parameters as figure 3. Notice the delocalization in space of the wave packet at the transition. Before and after the transition, the variances ΔQ^2 and ΔP^2 are small (compared to the distance between equilibrium points) showing localized states.

FIG. 5. Evolution in time of the mean position $\langle Q\rangle$ (lower curve) and momentum $\langle P\rangle$ (upper curve). Parameters same as figure 3. The mean is taken over 100 realizations. The time scale of the decay is much larger than the dissipative time of $1/\kappa = 0.67$.

FIG. 6. Simulation of an ideal (single) experiment according to the QSD model. Parameters are the same as in figure 1. The detuning step is 0.1 and the measurement time is $t_m = 50$. The dotted line represents the classical steady state excitation number.

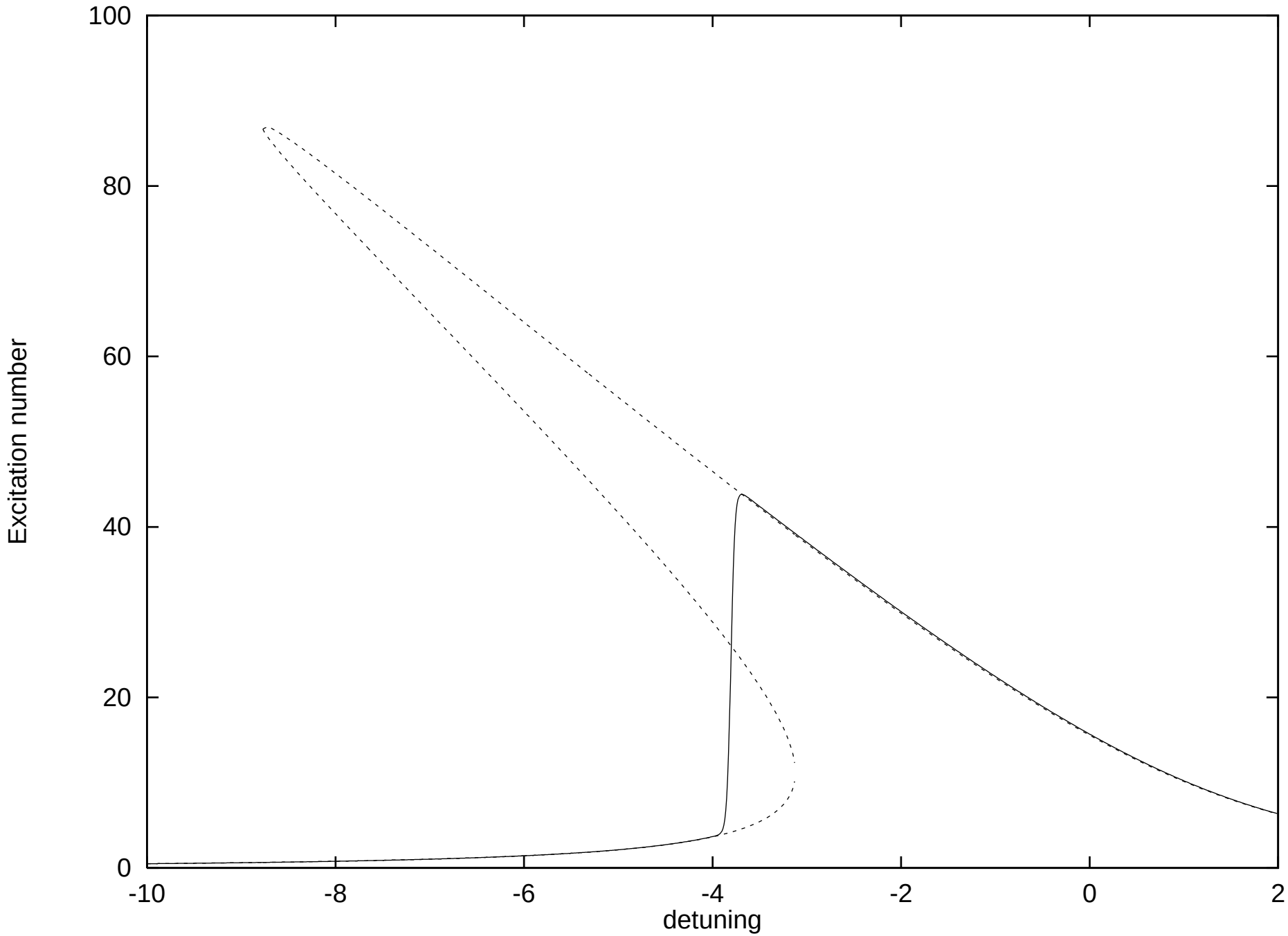
100
80
60
40
20
0
Excitation number
-10
-8
-6
-4
-2
0
2
detuning

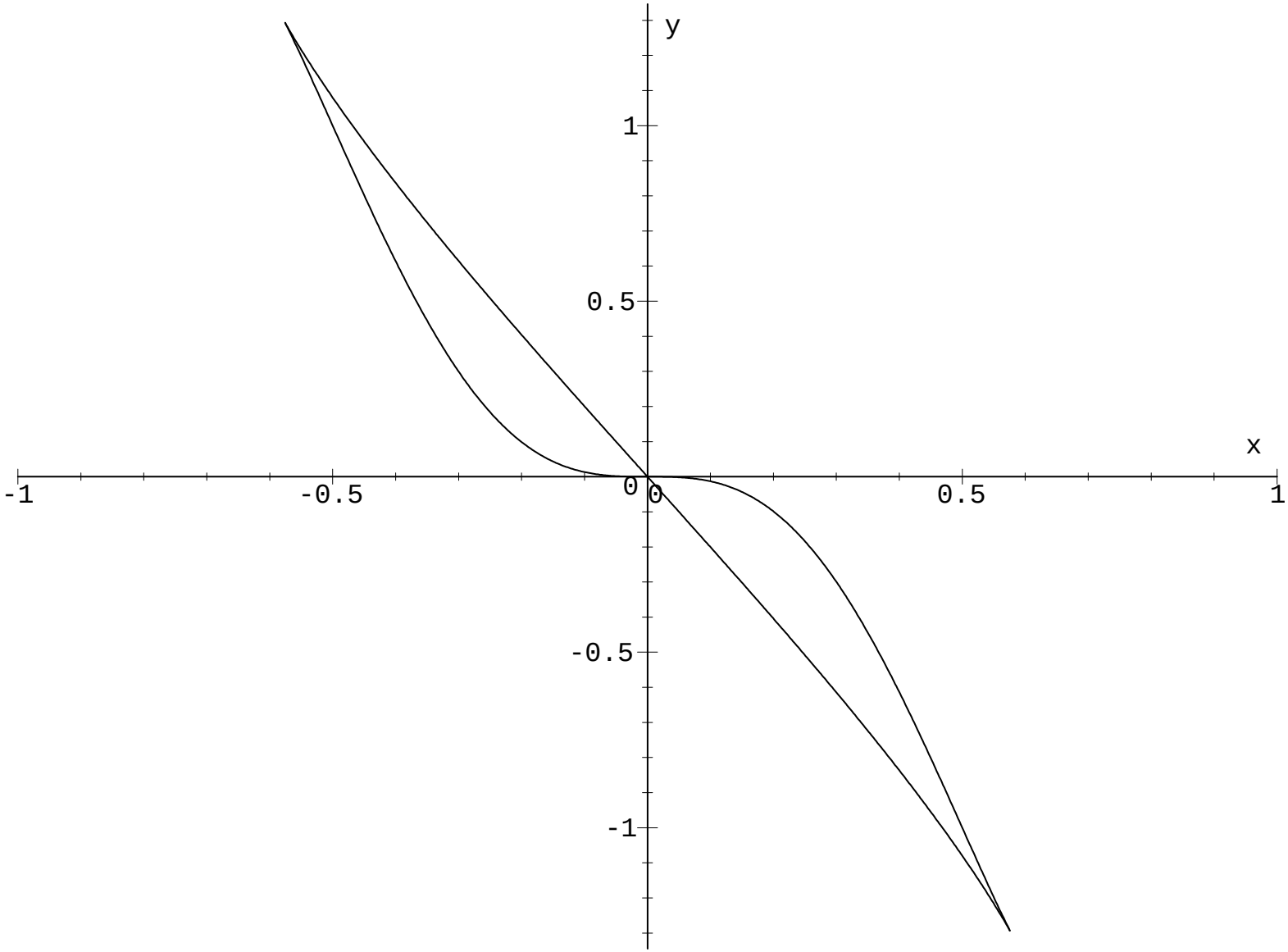
y
1
0.5
x
-1
-0.5
0
0
0.5
1
-0.5
-1

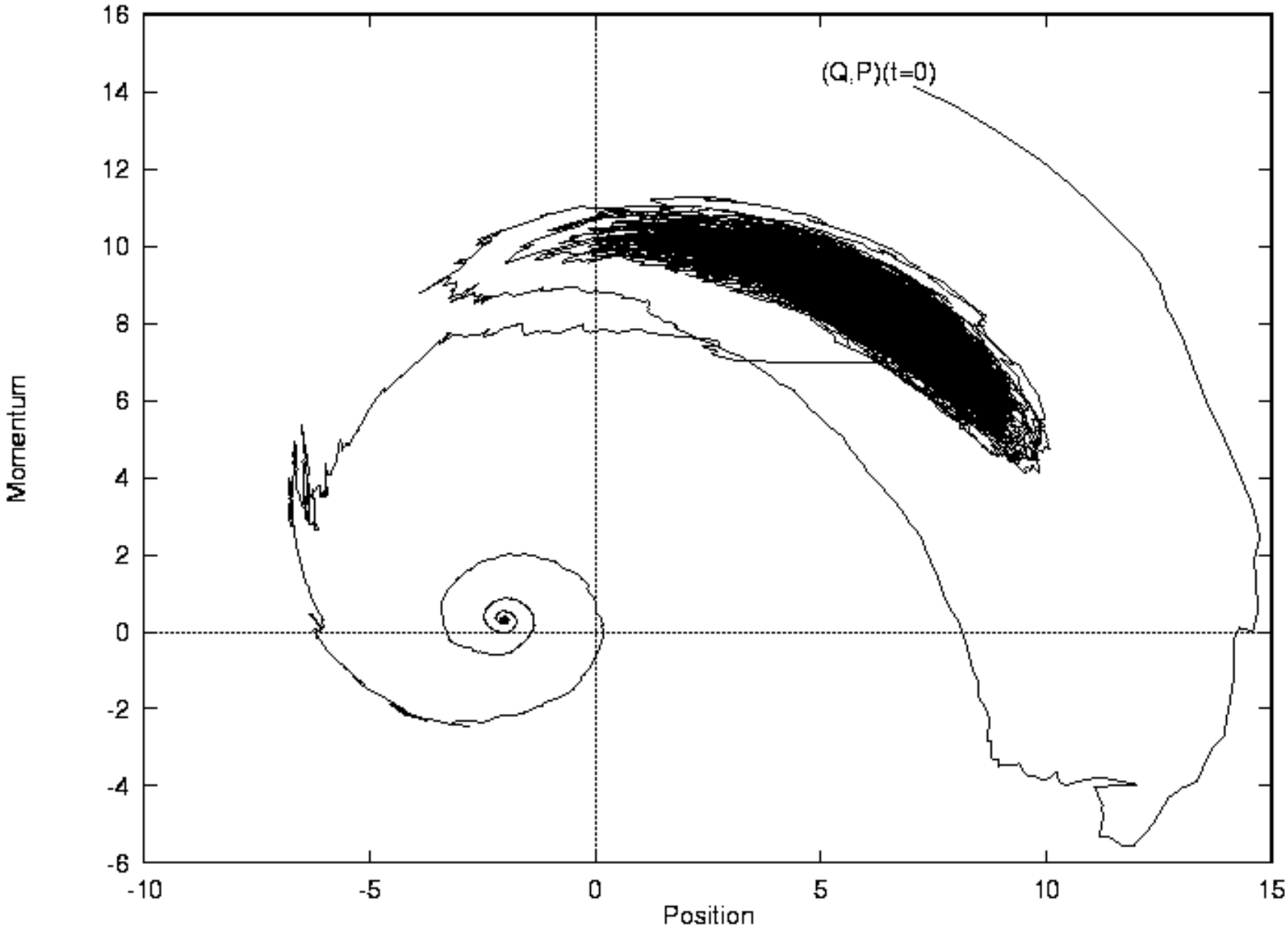

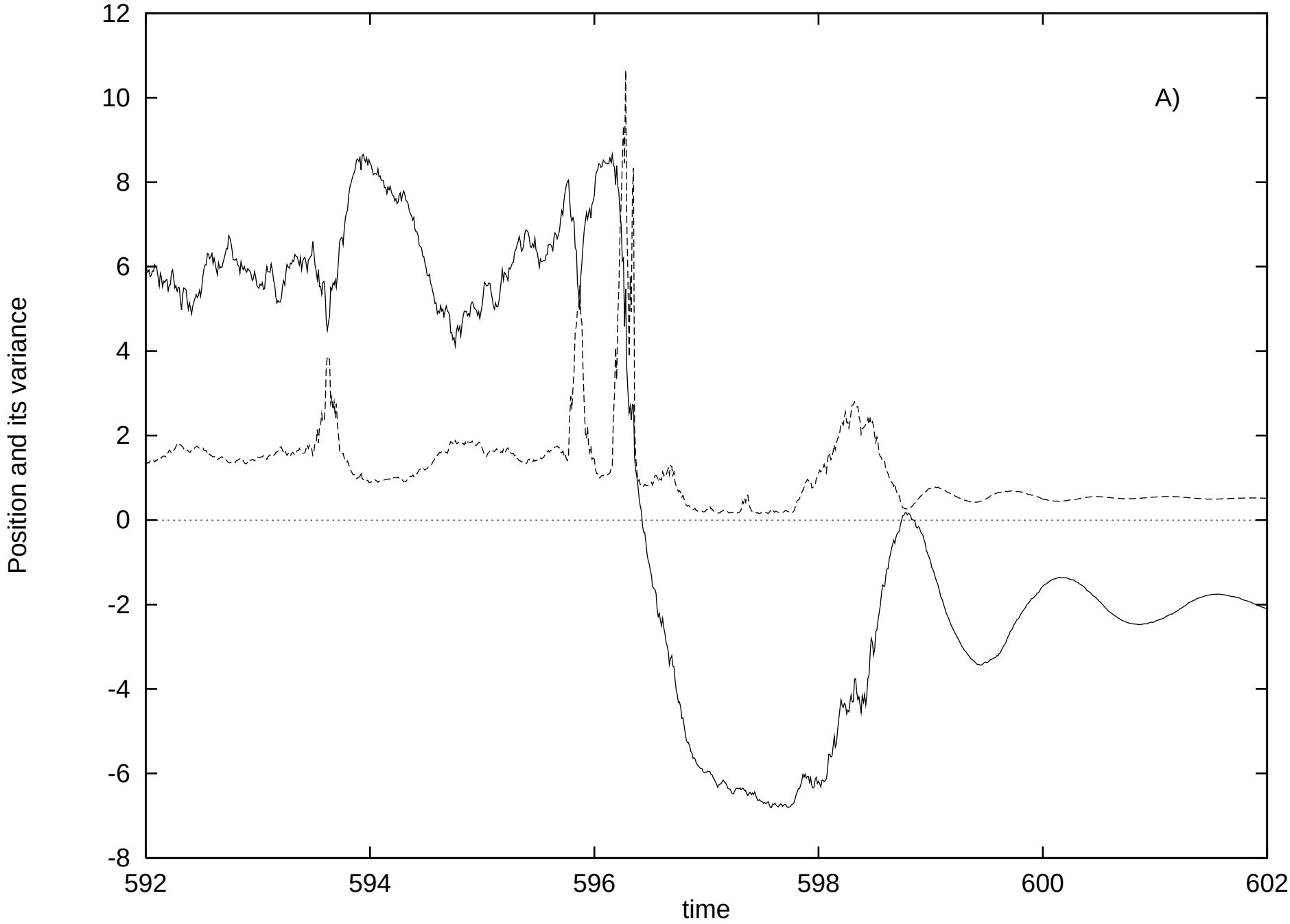
A)
Position and its variance
time
12
10
8
6
4
2
0
-2
-4
-6
-8
592
594
596
598
600
602

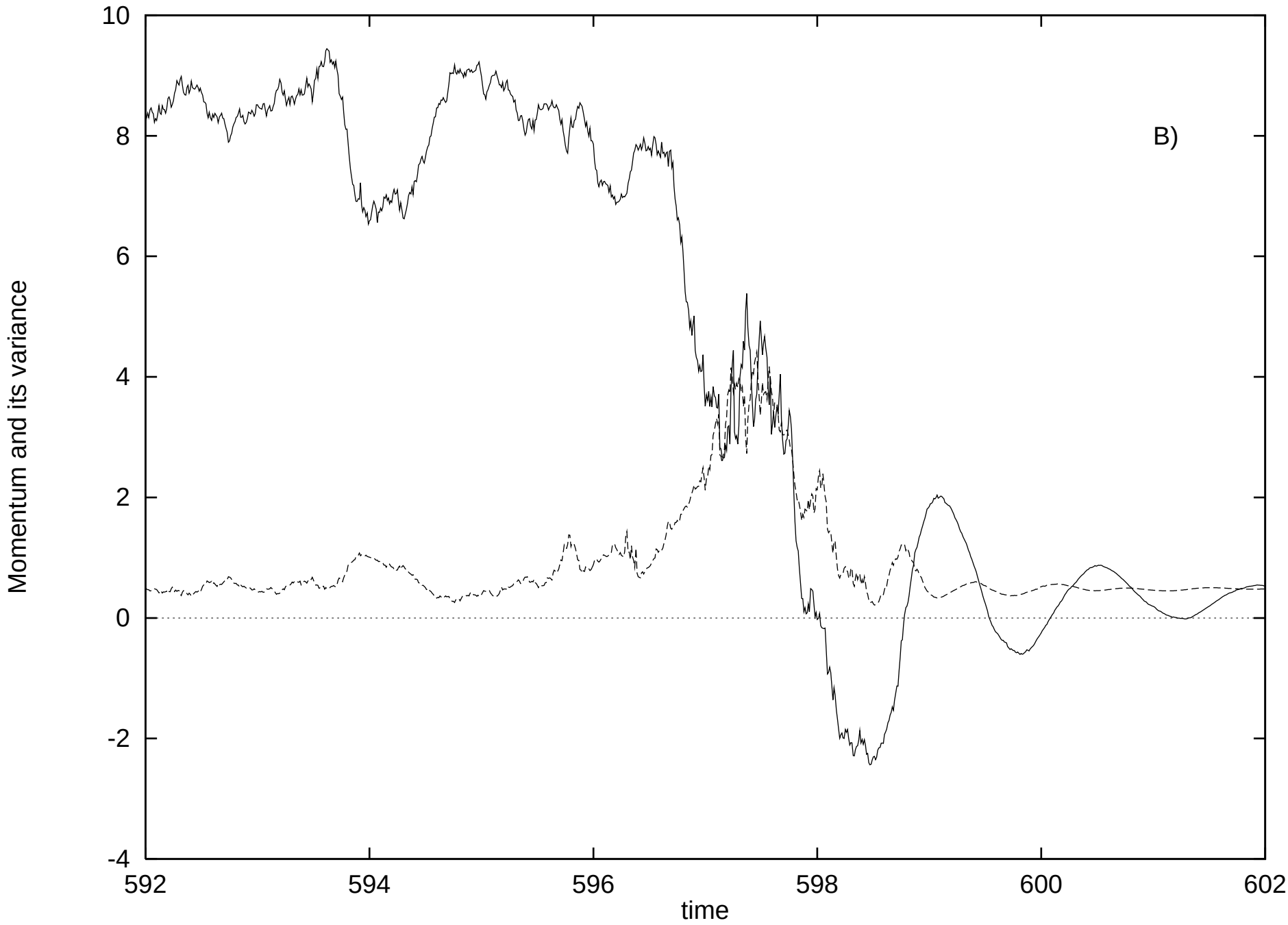
B)
Momentum and its variance
time
10
8
6
4
2
0
-2
-4
592
594
596
598
600
602

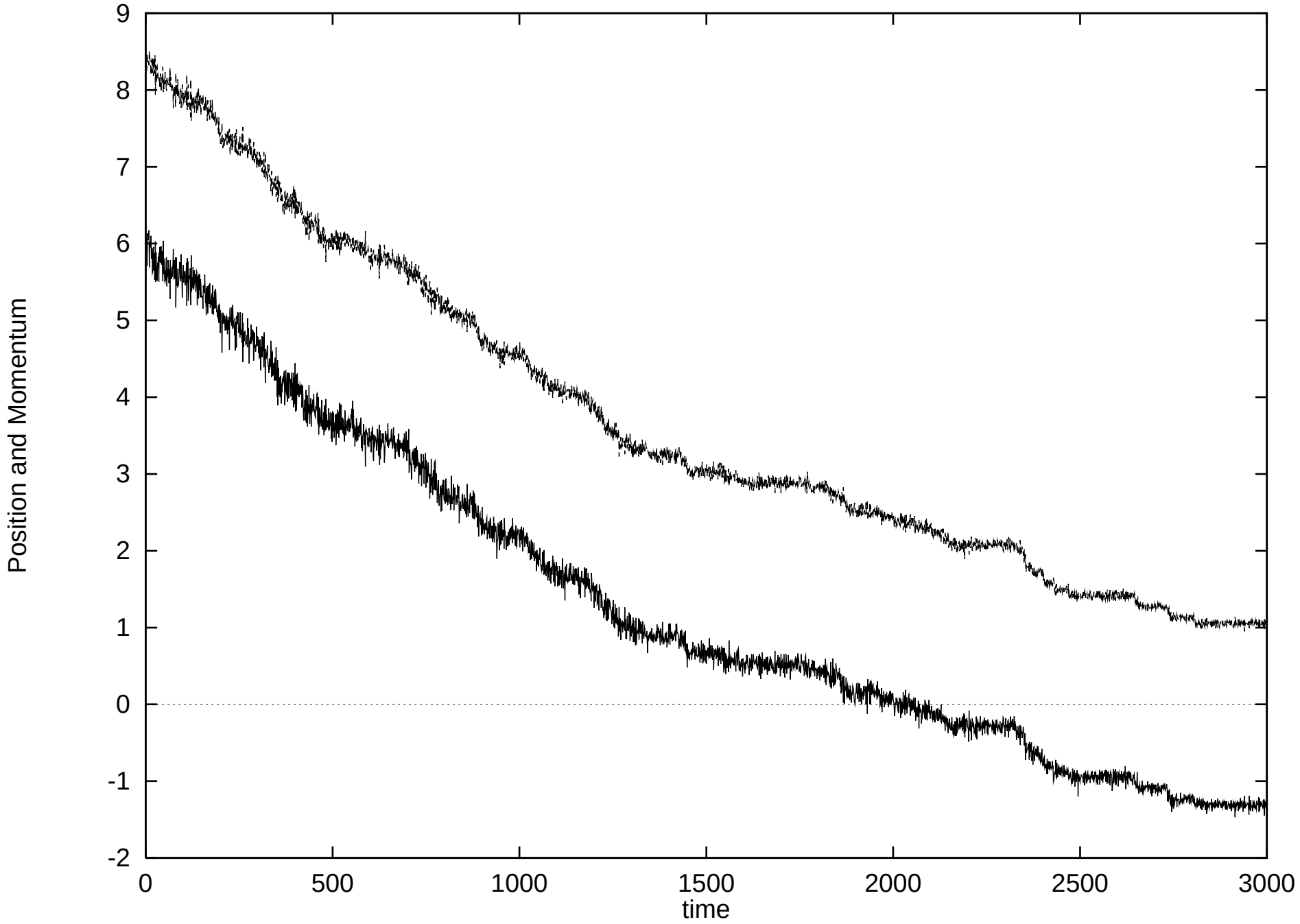
Position and Momentum
time
9
8
7
6
5
4
3
2
1
0
-1
-2
0
500
1000
1500
2000
2500
3000

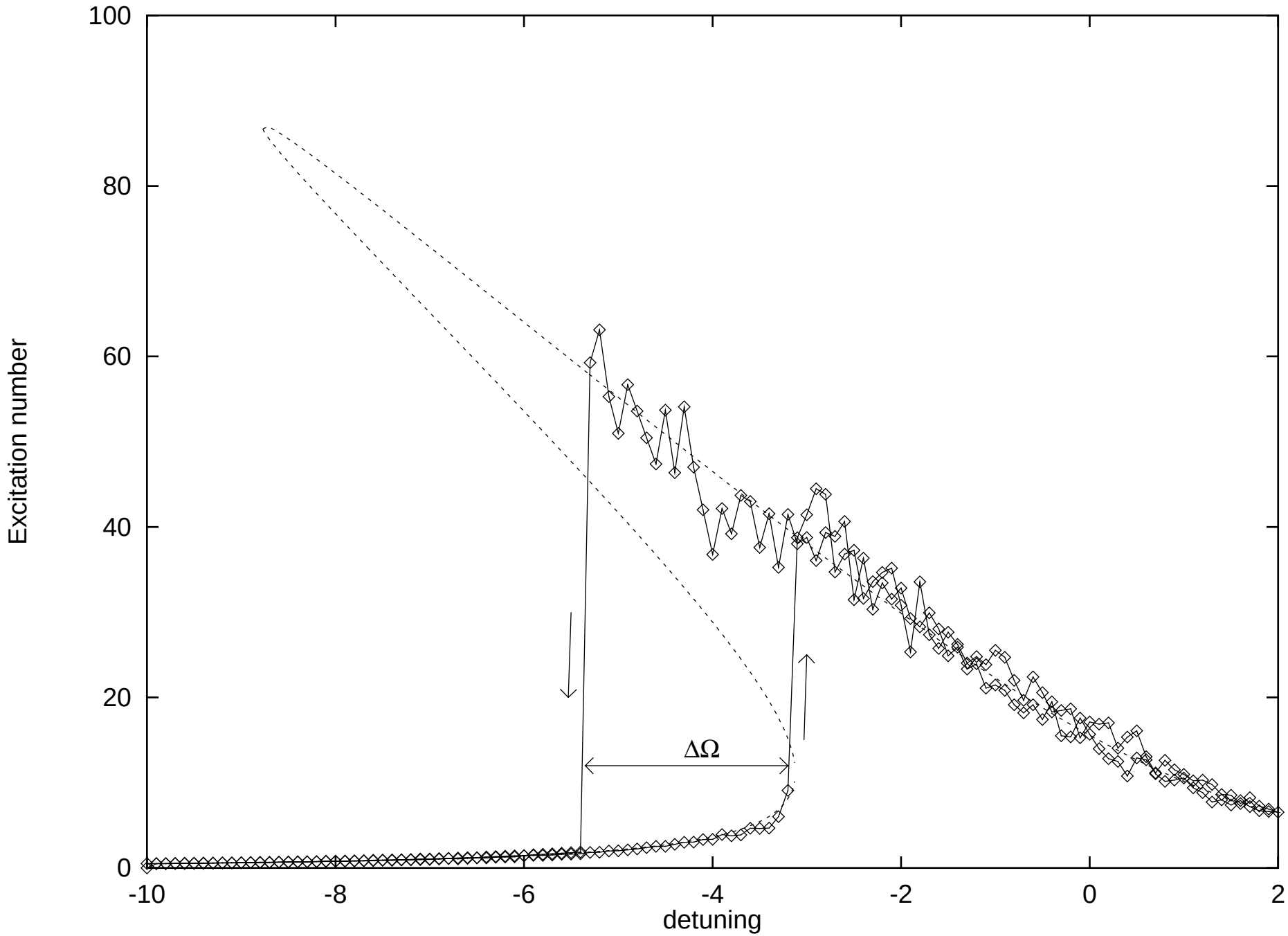
100
80
60
40
20
0
Excitation number
-10
-8
-6
-4
-2
0
2
detuning
ΔΩ